Acta Cryst E CRYSTALLOGRAPHIC COMMUNICATIONS

ISSN 2056-9890

A 1:1 solvate structure of succinonitrile and lithium thiocyanate

Christopher M. Burba[a]* and Douglas R. Powell[b]

[a]Department of Natural Sciences, Northeastern State University, 611 N. Grand Ave., Tahlequah, OK 74464, USA, and [b]Department of Chemistry and Biochemistry, University of Oklahoma, 101 Stephenson Parkway, Norman, OK 73019, USA. *Correspondence e-mail: burba@nsuok.edu

Received 5 October 2022
Accepted 18 November 2022

Edited by M. Zeller, Purdue University, USA

Keywords: lithium battery; plastic crystalline electrolyte; X-ray diffraction; crystal structure.

CCDC reference: 2220707

Supporting information: this article has supporting information at journals.iucr.org/e

A 1:1 solvate structure of succinonitrile and lithium thiocyanate, namely, *catena*-poly[lithium-di-μ-thiocyanato-lithium-di-μ-butanedinitrile], $[Li(NCS)(C_4H_4N_2)]_n$ or $LiSCN{\cdot}NC(CH_2)_2CN$, was isolated and its structure was solved. Lithium ions are tetrahedrally coordinated by two nitrile groups from separate succinonitrile molecules, as well as S and N atoms of separate SCN^- anions. The succinonitrile molecules and Li^+ ions form double-chain one-dimensional coordination polymers that are bridged by $Li_2(SCN)_2$ dimers. The coordination network extends along $[\bar{1}01]$. Weak hydrogen-bonding interactions are also noted among the constituent molecules.

1. Chemical context

Most commercial lithium-ion batteries employ liquid-phase electrolyte solutions that are composed of organic solvents and lithium salts. It is now well documented, however, that these materials can present consumer safety risks (Chen *et al.*, 2021). For example, internal electrical shortages may lead to thermal runaway and solvent combustion. The battery community has responded to this problem by pursuing safer alternatives to 'traditional' electrolyte solutions, such as all-solid-state polymer electrolytes (Armand, 1994; Zhou *et al.*, 2019). Despite the advantages provided by solid-state electrolytes, there are significant technological issues preventing their widespread commercialization (Zhou *et al.*, 2019). For example, lithium-ion batteries require highly conductive electrolyte systems ($>10^{-3}$ S cm^{-1}) to support rapid charging and discharging rates. This requirement is probably the most formidable challenge currently facing polymer electrolytes since most candidate materials simply do not have high enough ionic conductivities to be commercially competitive.

Alternative solid-state ion conductors, such as those created from plastic crystalline materials (Zhou *et al.*, 2019; Zhu *et al.*, 2019), are able to deliver high ionic conductivities without sacrificing mechanical integrity. Plastic crystalline materials possess long-range translational order with some degree of orientational or conformational disorder. Alarco and coworkers (2004) examined a family of plastic crystalline electrolytes based on succinonitrile, a highly polar compound (dielectric constant $\varepsilon = 66$; Williams & Smyth, 1962) capable of solvating lithium ions. These materials deliver good electrochemical performance and are promising candidates for lithium battery applications (Alarco *et al.*, 2004).

Our contribution to this field is the isolation and analysis of a solvate structure formed between lithium thiocyanate and

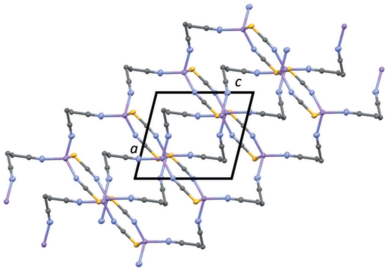

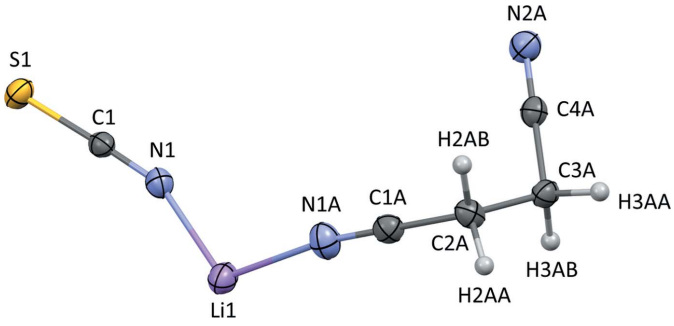

Figure 1
The asymmetric unit of $LiSCN{\cdot}NC(CH_2)_2CN$ solvate structure. Displacement ellipsoids are shown at the 50% probability level.

succinonitrile that we collected from a mixture of the two components. Additional details about the crystalline material and subsequent structure determination may be found in the *Synthesis and Crystallization* section. The crystallographic information reveals cation–solvent and cation–anion interaction motifs that may guide the design of next generation plastic crystalline electrolytes for lithium-ion battery applications.

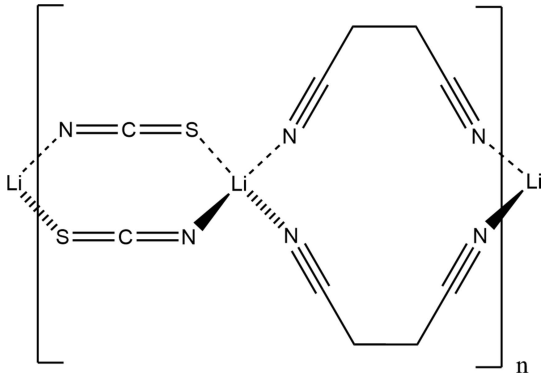

2. Structural commentary

The succinonitrile lithium thiocyanate solvate, $LiSCN{\cdot}NC(CH_2)_2CN$, belongs to the $P2_1/n$ space group with Z = 4. A displacement ellipsoid plot constituting the asymmetric unit with the atom-labeling scheme is shown in Fig. 1. Projections of the unit cell along the *a*, *b*, and *c* crystallographic axes are provided in Fig. 2, and the Li^+ coordination environment and cation–succinonitrile interactions are depicted in Fig. 3. Lithium ions are tetrahedrally coordinated in $LiSCN{\cdot}NC(CH_2)_2CN$. Two of the ligating N atoms originate from two different succinonitrile molecules, yielding one-dimensional coordination polymer chains composed of cations and succinonitrile. Each Li^+ ion is also coordinated by S and N atoms from two different thiocyanate anions to produce $Li_2(SCN)_2$ dimers that link adjacent lithium–succinonitrile polymer chains. The resulting double-chain network is oriented along $[\bar{1}01]$ (see Fig. 4).

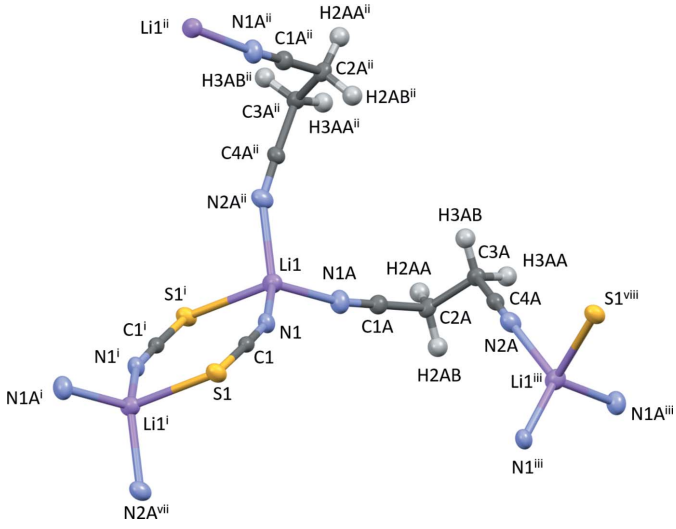

Figure 3
Coordination environments for Li^+, SCN^-, and succinonitrile with atom labeling. Symmetry codes: (i) $1-x, 1-y, 2-z$; (ii) $x-\frac{1}{2}, \frac{3}{2}-y, z+\frac{1}{2}$; (iii) $x+\frac{1}{2}, \frac{3}{2}-y, z-\frac{1}{2}$; (vii) $\frac{3}{2}-x, y-\frac{1}{2}, \frac{3}{2}-z$; (viii) $\frac{3}{2}-x, \frac{1}{2}+y, \frac{3}{2}-z$.

The cation–anion Li1—N1 bond [1.985 (3) Å] is shorter than either Li–N bond formed between Li^+ and the nitrile groups of succinonitrile [Li1—N1*A* = 2.028 (3) Å and Li1—N2*A*^{ii} = 2.093 (2) Å; symmetry code: (ii) $x-\frac{1}{2}, \frac{3}{2}-y, z+\frac{1}{2}$]. By way of comparison, Li1—S1^i is relatively longer at 2.572 (3) Å

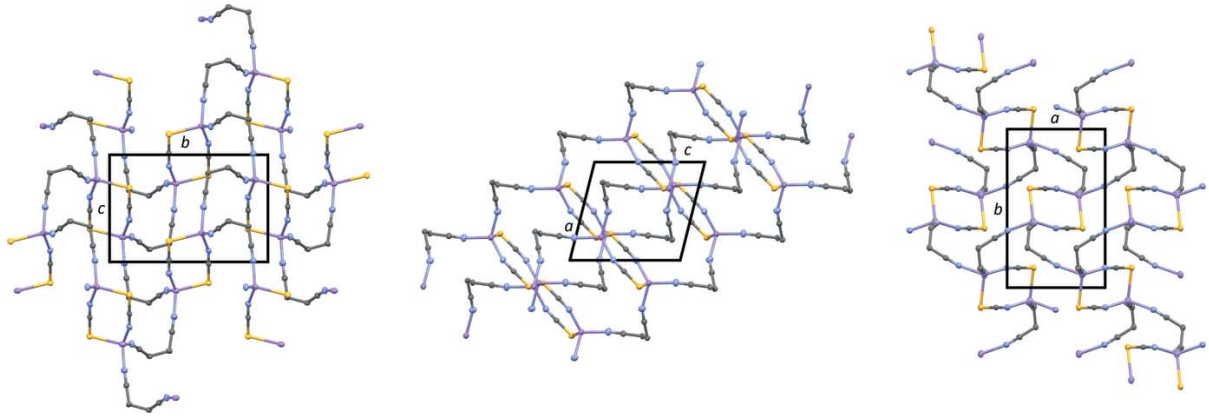

Figure 2
Projections of the unit cell for $LiSCN{\cdot}NC(CH_2)_2CN$ along the *a* (left), *b* (center), and *c* (right) axes. Hydrogen atoms are omitted for clarity.

Table 1
Hydrogen-bond geometry (Å, °).

D—H···A	D—H	H···A	D···A	D—H···A
C2A—H2AA···S1^{iv}	0.99	2.93	3.5212 (15)	120
C2A—H2AB···N1^{v}	0.99	2.63	3.4159 (17)	137
C3A—H3AA···N2A^{vi}	0.99	2.61	3.4232 (17)	140
C3A—H3AB···N1^{vi}	0.99	2.54	3.4257 (17)	150

Symmetry codes: (iv) $x-1, y, z-1$; (v) $x, y, z-1$; (vi) $x-\frac{1}{2}, -y+\frac{3}{2}, z-\frac{1}{2}$.

[symmetry code: (i) $1-x, 1-y, 2-z$]. The tetrahedral coordination environment about Li^+ is somewhat distorted with bond angles centered on the cation ranging from 125.75 (13) to 98.67 (9)°. The Li1—N1A—C1A bond angle approaches a linear geometry [170.60 (13)°], whereas Li1^{iii}—N2A—C4A is noticeably bent [155.39 (13)°; symmetry code: (iii) $x+\frac{1}{2}, \frac{3}{2}-y, z-\frac{1}{2}$]. By way of comparison, the Li1—N1—C1 and Li1—S1^{i}—C1^{i} bond angles are 159.26 (12) and 96.67 (6)°, respectively. The succinonitrile molecules adopt a *gauche* conformation with a 66.04 (13)° C1A—C2A—C3A—C4A torsion angle and comparable C≡N bond lengths. Both are similar to the low-temperature α phase of pure succinonitrile (Hore *et al.*, 2009; Whitfield, *et al.*, 2008).

3. Supramolecular features

Possible hydrogen bonds between C—H groups of succinonitrile and N or S atoms are detected in LiSCN·NC(CH$_2$)$_2$CN (Table 1). These interactions have relatively long distances and are of low directionality. Hence, we classify the hydrogen bonds as weak.

4. Database survey

The structure of the SCN^- anion in our solvate structure may be compared against the LiSCN·xH$_2$O (x = 0, 1, and 2) family of compounds. Joos *et al.* (2022) report crystallographic data for two phases of LiSCN·H$_2$O: a room-temperature phase with space group *C2/m* and a high-temperature phase with space group *Pnam*. The structures for LiSCN and LiSCN·2H$_2$O, both belonging to space group *Pnma*, are provided by Reckeweg *et al.* (2014). Structural parameters for the anions in these compounds are similar to each other and to LiSCN·NC(CH$_2$)$_2$CN. The C1═S1 and C1═N1 bond lengths in LiSCN·NC(CH$_2$)$_2$CN [1.646 (1) and 1.167 (2) Å, respectively] are comparable to those found in LiSCN (1.643 and 1.162 Å, respectively). Furthermore, the C1═N1 bond length is only slightly longer than those reported for the LiSCN hydrates (*e.g.*, the average length is 1.167 Å for LiSCN·xH$_2$O). Finally, the 178.0 (1)° S1—C1—N1 bond angle in LiSCN·NC(CH$_2$)$_2$CN only deviates slightly from a linear geometry and is closest in value to that found in LiSCN·2H$_2$O (177.55°).

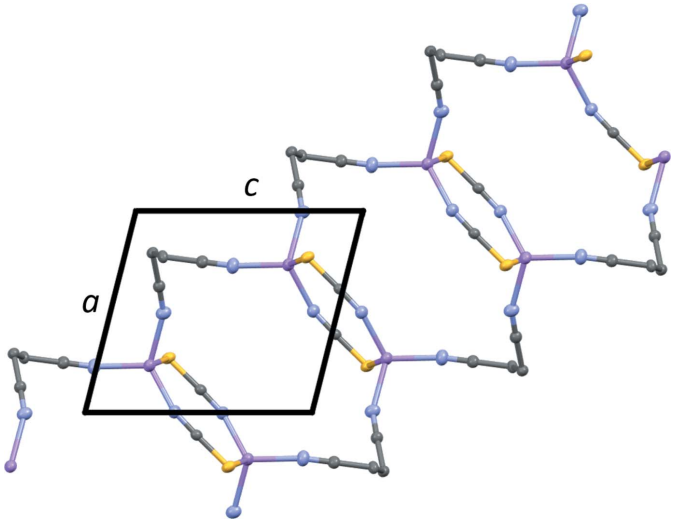

Figure 4
Double-chain structure of LiSCN·NC(CH$_2$)$_2$CN when viewed along the *b* axis. Hydrogen atoms are omitted for clarity.

Table 2
Experimental details.

Crystal data	
Chemical formula	[Li(NCS)(C$_4$H$_4$N$_2$)]
M_r	145.11
Crystal system, space group	Monoclinic, $P2_1/n$
Temperature (K)	100
a, b, c (Å)	7.5802 (13), 11.868 (3), 8.2724 (16)
β (°)	104.155 (7)
V (Å^3)	721.6 (3)
Z	4
Radiation type	Mo $K\alpha$
μ (mm^{-1})	0.36
Crystal size (mm)	0.37 × 0.27 × 0.27
Data collection	
Diffractometer	Area detector κ–geometry diffractometer
Absorption correction	Multi-scan (*SADABS*; Krause *et al.*, 2015)
T_{min}, T_{max}	0.403, 0.490
No. of measured, independent and observed [$I > 2\sigma(I)$] reflections	33422, 2400, 2210
R_{int}	0.097
(sin $\theta/\lambda)_{max}$ (Å^{-1})	0.735
Refinement	
$R[F^2 > 2\sigma(F^2)]$, $wR(F^2)$, S	0.049, 0.140, 1.04
No. of reflections	2400
No. of parameters	92
H-atom treatment	H-atom parameters constrained
$\Delta\rho_{max}$, $\Delta\rho_{min}$ (e Å^{-3})	0.41, −0.36

Computer programs: *APEX3* (Bruker, 2018), *SAINT* (Bruker, 2016), *SHELXT2014/5* (Sheldrick, 2015*a*), *SHELXL2018/3* (Sheldrick, 2015*b*), and *Mercury* (Macrae *et al.*, 2020).

5. Synthesis and crystallization

Succinonitrile (NC(CH$_2$)$_2$CN, CAS# 110–61-2) and lithium thiocyanate hydrate (LiSCN·xH$_2$O, CAS# 123333–85-7) were both obtained from Sigma Aldrich. The LiSCN·xH$_2$O was dehydrated in a vacuum oven. The two reagents were then stored inside a <1 p.p.m. H$_2$O, argon-filled dry box. A total of 0.3005 g of LiSCN was mixed with 0.5550 g of succinonitrile, and gentle heating on a hot plate promoted dissolution of the salt into the solvent. The resulting solution was stored under

argon gas until crystals of sufficient size formed. A colorless, block-shaped crystal of dimensions 0.272 mm × 0.274 mm × 0.368 mm was selected for structural analysis.

6. Refinement

Crystal data, data collection, and structure refinement details are summarized in Table 2. The positions of hydrogen atoms bonded to carbon atoms were initially determined by geometry and were refined using a riding model. Non-hydrogen atoms were refined with anisotropic displacement parameters. Hydrogen atom displacement parameters were set to 1.2 times the isotropic equivalent displacement parameters of the bonded atoms.

Acknowledgements

The authors thank Northeastern State University for access to facilities needed to prepare the crystals. The authors declare no competing financial interests.

Funding information

Funding for this research was provided by: National Science Foundation (grant No. CHE-1726630).

References

Alarco, P.-J., Abu-Lebdeh, Y., Abouimrane, A. & Armand, M. (2004). *Nat. Mater.* **3**, 476–481.
Armand, M. (1994). *Solid State Ionics*, **69**, 309–319.
Bruker (2016). *SAINT*. Bruker Nano Inc., Madison, Wisconsin, USA.
Bruker (2018). *APEX3*. Bruker Nano Inc., Madison, Wisconsin, USA.
Chen, Y., Kang, Y., Zhao, Y., Wang, L., Liu, J., Li, Y., Liang, Z., He, X., Li, X., Tavajohi, N. & Li, B. (2021). *J. Energy Chem.*, **59**, 83-99.
Hore, S., Dinnebier, R., Wen, W., Hanson, J. & Maier, J. (2009). *Z. Anorg. Allg. Chem.* **635**, 88–93.
Joos, M., Conrad, M., Bette, S., Merkle, R., Dinnebier, R. E., Schleid, T. & Maier, J. (2022). *J. Phys. Chem. Solids*, **160**, 110299.
Krause, L., Herbst-Irmer, R., Sheldrick, G. M. & Stalke, D. (2015). *J. Appl. Cryst.* **48**, 3–10.
Macrae, C. F., Sovago, I., Cottrell, S. J., Galek, P. T. A., McCabe, P., Pidcock, E., Platings, M., Shields, G. P., Stevens, J. S., Towler, M. & Wood, P. A. (2020). *J. Appl. Cryst.* **53**, 226–235.
Reckeweg, O., Schulz, A., Blaschkowski, B., Schleid, T. & DiSalvo, F. J. (2014). *Z. Naturforsch.* **69**, 17–24.
Sheldrick, G. M. (2015*a*). *Acta Cryst.* A**71**, 3–8.
Sheldrick, G. M. (2015*b*). *Acta Cryst.* C**71**, 3–8.
Whitfield, P. S., Le Page, Y., Abouimrane, A. & Davidson, I. J. (2008). *Powder Diffr.* **23**, 292–299.
Williams, D. E. & Smyth, C. P. (1962). *J. Am. Chem. Soc.* **84**, 1808–1812.
Zhou, D., Shanmukaraj, D., Tkacheva, A., Armand, M. & Wang, G. (2019). *Chem*, **5**, 2326–2352.
Zhu, H., MacFarlane, D. R., Pringle, J. M. & Forsyth, M. (2019). *Trends Chem.* **1**, 126–140.

supporting information

Acta Cryst. (2022). E**78**, 1284-1287 [https://doi.org/10.1107/S2056989022011094]

A 1:1 solvate structure of succinonitrile and lithium thiocyanate

Christopher M. Burba and Douglas R. Powell

Computing details

Data collection: *APEX3* (Bruker, 2018); cell refinement: *SAINT* (Bruker, 2016); data reduction: *SAINT* (Bruker, 2016); program(s) used to solve structure: *SHELXT2014/5* (Sheldrick, 2015a); program(s) used to refine structure: *SHELXL2018/3* (Sheldrick, 2015b); molecular graphics: *Mercury* (Macrae *et al.*, 2020); software used to prepare material for publication: *SHELXL2018/3* (Sheldrick, 2015b).

catena-Poly[lithium-di-μ-thiocyanato-lithium-di-μ-butanedinitrile]

Crystal data

$[Li(NCS)(C_4H_4N_2)]$
$M_r = 145.11$
Monoclinic, $P2_1/n$
$a = 7.5802$ (13) Å
$b = 11.868$ (3) Å
$c = 8.2724$ (16) Å
$\beta = 104.155$ (7)°
$V = 721.6$ (3) Å^3
$Z = 4$
$F(000) = 296$
$D_x = 1.336$ Mg m^{-3}
Mo $K\alpha$ radiation, $\lambda = 0.71073$ Å
Cell parameters from 8809 reflections
$\theta = 2.8$–$33.7°$
$\mu = 0.36$ mm^{-1}
$T = 100$ K
Block, colourless
0.37 × 0.27 × 0.27 mm

Data collection

Area detector κ–geometry diffractometer
Radiation source: microfocus sealed tube, Incoatec IμS 3.0
Multilayer mirror monochromator
ω and φ scans
Absorption correction: multi-scan (SADABS; Krause *et al.*, 2015)
$T_{min} = 0.403$, $T_{max} = 0.490$
33422 measured reflections
2400 independent reflections
2210 reflections with $I > 2\sigma(I)$
$R_{int} = 0.097$
$\theta_{max} = 31.5°$, $\theta_{min} = 3.1°$
$h = -11 \rightarrow 11$
$k = -17 \rightarrow 17$
$l = -12 \rightarrow 12$

Refinement

Refinement on F^2
Least-squares matrix: full
$R[F^2 > 2\sigma(F^2)] = 0.049$
$wR(F^2) = 0.140$
$S = 1.04$
2400 reflections
92 parameters
0 restraints
Primary atom site location: shelxt
Secondary atom site location: difference Fourier map
Hydrogen site location: inferred from neighbouring sites
H-atom parameters constrained
$w = 1/[\sigma^2(F_o^2) + (0.0936P)^2 + 0.2195P]$ where $P = (F_o^2 + 2F_c^2)/3$
$(\Delta/\sigma)_{max} = 0.001$
$\Delta\rho_{max} = 0.41$ e Å^{-3}
$\Delta\rho_{min} = -0.36$ e Å^{-3}

Extinction correction: *SHELXL2018/3* (Sheldrick 205b8), $Fc^{*}=kFc[1+0.001xFc^{2}\lambda^{3}/\sin(2\theta)]^{-1/4}$
Extinction coefficient: 0.044 (16)

Special details

Geometry. All esds (except the esd in the dihedral angle between two l.s. planes) are estimated using the full covariance matrix. The cell esds are taken into account individually in the estimation of esds in distances, angles and torsion angles; correlations between esds in cell parameters are only used when they are defined by crystal symmetry. An approximate (isotropic) treatment of cell esds is used for estimating esds involving l.s. planes.

Fractional atomic coordinates and isotropic or equivalent isotropic displacement parameters (Å²)

	x	*y*	*z*	U_{iso}*/U_{eq}
S1	0.76963 (4)	0.62537 (2)	1.19303 (4)	0.02384 (15)
N1	0.49689 (16)	0.62469 (8)	0.89339 (15)	0.0233 (2)
C1	0.61234 (16)	0.62517 (8)	1.01617 (15)	0.0184 (2)
Li1	0.2669 (3)	0.5822 (2)	0.7318 (3)	0.0262 (4)
N1A	0.27232 (17)	0.59303 (10)	0.48836 (14)	0.0290 (3)
N2A	0.50670 (16)	0.86047 (9)	0.23500 (16)	0.0267 (2)
C1A	0.25268 (17)	0.60611 (10)	0.34831 (16)	0.0220 (2)
C2A	0.22707 (18)	0.62314 (9)	0.16912 (15)	0.0208 (2)
H2AA	0.116761	0.582051	0.109166	0.025*
H2AB	0.332380	0.590928	0.134143	0.025*
C3A	0.20743 (15)	0.74810 (10)	0.11935 (14)	0.0210 (2)
H3AA	0.174675	0.753955	−0.003771	0.025*
H3AB	0.107091	0.781563	0.160645	0.025*
C4A	0.37413 (15)	0.81229 (9)	0.18592 (14)	0.0207 (2)

Atomic displacement parameters (Å²)

	U^{11}	U^{22}	U^{33}	U^{12}	U^{13}	U^{23}
S1	0.0196 (2)	0.0238 (2)	0.0247 (2)	0.00019 (8)	−0.00112 (13)	0.00022 (9)
N1	0.0244 (5)	0.0225 (5)	0.0225 (5)	−0.0005 (3)	0.0045 (4)	0.0044 (3)
C1	0.0176 (5)	0.0168 (5)	0.0218 (5)	0.0005 (3)	0.0067 (4)	0.0020 (3)
Li1	0.0232 (10)	0.0341 (11)	0.0204 (9)	0.0029 (8)	0.0034 (7)	0.0021 (8)
N1A	0.0357 (6)	0.0275 (5)	0.0231 (5)	−0.0024 (4)	0.0061 (4)	0.0007 (4)
N2A	0.0249 (5)	0.0210 (4)	0.0318 (6)	−0.0011 (4)	0.0021 (4)	0.0008 (4)
C1A	0.0227 (5)	0.0210 (5)	0.0220 (5)	−0.0022 (4)	0.0049 (4)	−0.0018 (4)
C2A	0.0231 (5)	0.0229 (5)	0.0174 (5)	−0.0043 (4)	0.0068 (4)	−0.0040 (3)
C3A	0.0180 (4)	0.0260 (5)	0.0180 (5)	−0.0006 (4)	0.0022 (4)	0.0000 (4)
C4A	0.0219 (5)	0.0191 (5)	0.0204 (5)	0.0022 (4)	0.0043 (4)	0.0010 (3)

Geometric parameters (Å, º)

S1—C1	1.6459 (13)	C1A—C2A	1.4611 (17)
S1—Li1^{i}	2.572 (3)	C2A—C3A	1.5366 (17)
N1—C1	1.1674 (18)	C2A—H2AA	0.9900
N1—Li1	1.985 (3)	C2A—H2AB	0.9900

Li1—N1A	2.028 (3)	C3A—C4A	1.4628 (16)
Li1—N2A^{ii}	2.093 (2)	C3A—H3AA	0.9900
N1A—C1A	1.1420 (17)	C3A—H3AB	0.9900
N2A—C4A	1.1411 (16)		
C1—S1—Li1^{i}	96.67 (6)	C1A—C2A—H2AA	109.1
C1—N1—Li1	159.26 (12)	C3A—C2A—H2AA	109.1
N1—C1—S1	177.99 (11)	C1A—C2A—H2AB	109.1
N1—Li1—N1A	115.14 (12)	C3A—C2A—H2AB	109.1
N1—Li1—N2A^{ii}	125.75 (13)	H2AA—C2A—H2AB	107.8
N1A—Li1—N2A^{ii}	103.89 (11)	C4A—C3A—C2A	112.56 (10)
N1—Li1—S1^{i}	102.07 (9)	C4A—C3A—H3AA	109.1
N1A—Li1—S1^{i}	109.28 (11)	C2A—C3A—H3AA	109.1
N2A^{ii}—Li1—S1^{i}	98.67 (9)	C4A—C3A—H3AB	109.1
C1A—N1A—Li1	170.60 (13)	C2A—C3A—H3AB	109.1
C4A—N2A—Li1^{iii}	155.39 (13)	H3AA—C3A—H3AB	107.8
N1A—C1A—C2A	179.80 (16)	N2A—C4A—C3A	177.96 (13)
C1A—C2A—C3A	112.68 (10)		
C1A—C2A—C3A—C4A	66.04 (13)		

Symmetry codes: (i) −*x*+1, −*y*+1, −*z*+2; (ii) *x*−1/2, −*y*+3/2, *z*+1/2; (iii) *x*+1/2, −*y*+3/2, *z*−1/2.

Hydrogen-bond geometry (Å, º)

D—H···*A*	*D*—H	H···*A*	*D*···*A*	*D*—H···*A*
C2*A*—H2*AA*···S1^{iv}	0.99	2.93	3.5212 (15)	120
C2*A*—H2*AB*···N1^{v}	0.99	2.63	3.4159 (17)	137
C3*A*—H3*AA*···N2*A*^{vi}	0.99	2.61	3.4232 (17)	140
C3*A*—H3*AB*···N1^{vi}	0.99	2.54	3.4257 (17)	150

Symmetry codes: (iv) *x*−1, *y*, *z*−1; (v) *x*, *y*, *z*−1; (vi) *x*−1/2, −*y*+3/2, *z*−1/2.